Ref.TH.1605-CERN

A RESONANCE MODEL FOR DEEP INELASTIC ELECTRON PROTON SCATTERING AND ELECTRON POSITRON ANNIHILATION

H.D. Dahmen *) and F. Steiner **)

CERN - Geneva

ABSTRACT

A resonance model for deep inelastic ep scattering and e^+e^- annihilation is studied making use of a generalized crossing relation. Scaling in deep annihilation is predicted and the scaling function $\bar{F}_2$ in this region is given. The multiplicity stays finite in this model except for the limiting case of vanishing slope of the trajectory of the resonance widths where the multiplicity grows logarithmically.

---

*) On leave of absence from Institut für Theoretische Physik, Universität Heidelberg and Kernforschungszentrum, Karlsruhe.

**) On leave of absence from Institut für Theoretische Kernphysik, Universität Karlsruhe.

Ref.TH.1605-CERN

22 December 1972

In a previous paper [1] locality and spectrum properties have been used to propose representations for the scaling functions of deep inelastic electron scattering and electron positron annihilation. In particular, a generalized crossing relation among the scaling functions of the two processes was obtained.

In the present note we start from a resonance model for the structure function $W_2(q^2, \nu)$, [2] $\nu = p\cdot q$, for deep inelastic electron proton scattering

$$e + p \longrightarrow e' + \text{"anything"}, \tag{1}$$

and predict with the help of the generalized crossing relation of Ref. 1) the scaling function $\bar{F}_2(\omega)$ for the deep electron positron annihilation

$$e + \bar{e}' \longrightarrow p + \text{"anything"}. \tag{2}$$

Resonance models for the process (1) have been proposed by several authors [3)-6)]. The papers referred to under 4), 5) and 6) show that an infinite set of resonances on a linearly rising Regge trajectory is able to produce the observed scaling. In particular, the models discussed in Refs. 5) and 6) reproduce the qualitative features of the experimental data even though they treat W_2 like a structure function in a scalar theory. Because of this observation and for reasons of simplicity we treat W_2 the same way, and saturate the triple discontinuity $g_2(q^2,Q^2,s,0)$, Eq. (4) of Ref. 1), of the virtual Compton amplitude by an infinite sum over narrow resonances *) in the s channel (see Fig. 1)

$$g_2(q^2, Q^2, s, 0) = \sum_{k=1}^{\infty} \operatorname{Im} G_k(q^2) \operatorname{Im} G_k(Q^2) \delta(s - M_k^2). \tag{3}$$

Here, $G_k(q^2)$ is the electromagnetic excitation form factor of the k^{th} resonance with mass M_k. The resonance masses lie on a linear Regge trajectory with slope α', i.e.,

$$M_k^2 = \alpha'^{-1} k + M_0^2. \tag{4}$$

---

*) The restriction to narrow resonances is not essential.

In order to ensure the correct threshold behaviour at $\omega = 1$ of the scaling function $F_2(\omega)$ for the process (1) the asymptotic decrease of the form factors $G_k(q^2)$ has to be that of dipoles [7]. Since, in addition, we have to avoid unphysical poles in the annihilation region the resonance poles dominating the form factors have to appear as conjugate pairs in the second sheet of $G_k(q^2)$. These two requirements lead us to the following ansatz for the imaginary parts *)

$$\operatorname{Im} G_k(q^2) = \theta(q^2-q_{sk}^2)\, N'' m_k^3 \frac{\partial}{\partial q^2} \frac{\gamma_k \Gamma_k}{(q^2-m_k^2)^2 + m_k^2 \Gamma_k^2} , \qquad (5)$$

N'' is a normalization constant of dimension $(\text{mass})^2$. Also the resonances of mass m_k dominating the form factors are assumed to lie on a linear trajectory

$$m_k^2 = \alpha'^{-1} k + m_0^2 . \qquad (6)$$

The squares of the total widths Γ_k are supposed to follow a linear increase

$$\Gamma_k^2 = \gamma' k + \Gamma_0^2 , \qquad (7)$$

whereas the "partial widths" γ_k should exhibit the zero of the imaginary part at the physical threshold **) $q_{sk}^2 = (M+M_k)^2$

$$\gamma_k = \frac{q^2 - q_{sk}^2}{q^2} \Gamma_k . \qquad (8)$$

---

*) The discontinuity across the unphysical cut below q_{sk}^2 has been neglected since this cut carries over into the unphysical region $-\infty < \omega < 0$ of the scaling function $F_2(\omega)$.

**) In order to keep the calculation as simple as possible we have put a first order zero in Eq. (8). Possible modifications of ansatz (8) taking into account the effect of an interaction radius have been tried and were found to give no essential improvement.

With these assumptions the triple discontinuity g_2, Eq. (3), scales like

$$\lim_{\substack{s\to\infty \\ \frac{q^2}{s},\frac{Q^2}{s}\ \text{fixed}}} \alpha' s\, g_2(q^2, Q^2, s, 0) = \psi\left(\frac{q^2}{s}, \frac{Q^2}{s}\right), \tag{9}$$

where the double spectral function $\psi(x,y)$ is given by

$$\psi(x,y) = N'^2\,\theta(x-1)\,\theta(y-1)\,\frac{\partial\phi}{\partial x}(x)\,\frac{\partial\phi}{\partial y}(y), \qquad N' = N''\alpha' \varkappa^2 \tag{10}$$

with

$$\phi(x) = \frac{x-1}{x\left[(x-1)^2+\varkappa^2\right]}, \qquad \varkappa^2 = \alpha'\gamma'. \tag{11}$$

In the derivation of the above result we have replaced the infinite sum in Eq. (3) by an integral over k extending from one to infinity.

For the scaling function $F(\omega)$ defined by

$$W_2(q^2,\nu) \xrightarrow[\substack{(-q^2)\to\infty \\ \omega\ \text{fixed}}]{} \frac{M^2}{(-q^2)}\,F(\omega) \tag{12}$$

with $\omega = -2\nu/q^2$, we derived in Ref. 1) the following representation

$$F(\omega) = \frac{1}{\omega-1}\,\frac{1}{\pi^3}\int_0^\infty dx \int_0^\infty dy\, \frac{\psi(x,y)}{\left(x+\frac{1}{\omega-1}\right)\left(y+\frac{1}{\omega-1}\right)}. \tag{13}$$

Thus, we obtain for the deep inelastic scaling function $F_2(\omega)$, defined by

$$\frac{\nu}{M^2} W_2(q^2, \nu) \xrightarrow[\substack{(-q^2)\to\infty \\ \omega \text{ fixed}}] \quad F_2(\omega) , \tag{14}$$

the result $(1 \leq \omega < \infty)$

$$F_2(\omega) = \frac{\omega}{\omega - 1} \frac{1}{2\pi^3} \int_0^\infty dx \int_0^\infty dy \frac{\psi(x,y)}{\left(x + \frac{1}{\omega-1}\right)\left(y + \frac{1}{\omega-1}\right)} . \tag{15}$$

With Eqs. (10) and (11) for the double spectral function ψ we get

$$F_2(\omega) = N^2 \Omega^3 f(x, \Omega) , \qquad \begin{pmatrix} 1 \leq \omega < \infty \\ 0 \leq \Omega < 1 \end{pmatrix} \tag{16}$$

where

$$N^2 = \frac{N'^2}{2\pi^3 (1 + x^2)^2} , \qquad \Omega = \frac{\omega - 1}{\omega} \tag{17}$$

and

$$f(x, \Omega) = \left\{ \frac{\Omega - 1 - \ln \Omega}{(\Omega - 1)^2} + \right. \tag{18}$$

$$\left. + \frac{1}{(1 + x^2\Omega^2)^2} \left[(1 - 2x^2\Omega - x^2\Omega^2)(1 + \ln x\Omega) + x\left(x\Omega - \frac{\pi}{2}\right)(1 + 2\Omega - x^2\Omega^2) \right] \right\}^2 .$$

For deep annihilation (2) we define the scaling function $\bar{F}_2(\omega)$ in the limit $q^2 \to \infty$ analogously to Eq. (14) with barred quantities. From the generalized crossing relation, Eq. (14), Ref.1), one reads off for $\bar{F}_2$

$$\bar{F}_2(\omega) = - \mathrm{Re}\, F_2(-\omega) + \frac{\omega}{\pi(1+\omega)} \psi\left(\frac{1}{1+\omega}, \frac{1}{1+\omega}\right) , \quad (-1 \leq \omega \leq 0) . \tag{19}$$

Using Eq. (16), we obtain for the scaling function $\bar{F}_2(-\omega)$ in the deep annihilation region

$$\bar{F}_2(-\omega) = N^2 |\Omega|^3 \bar{f}(x,\Omega), \quad \begin{pmatrix} 0 \le \omega \le 1 \\ -\infty < \Omega \le 0 \end{pmatrix},$$

$$\bar{f}(x,\Omega) = h(x,\Omega) + \pi^2 (1+x^2)^2 \Omega^2 \left\{ \frac{x^2\Omega^3 - \Omega + 2}{(\Omega-1)^2(1+x^2\Omega^2)^2} \right\}^2 . \tag{20}$$

Here $h(x,\Omega)$ is obtained from $f(x,\Omega)$ by replacing $\ln\Omega$ by $\ln|\Omega|$ in Eq. (18).

Now, we come to the discussion of the results.

1) In this model scaling also occurs in the annihilation region.

2) Obviously, the scaling functions $F_2(\omega)$ and $\bar{F}_2(-\omega)$, Eqs. (16) and (20), are positive in their physical domains.

3) $F_2(\omega)$ has a logarithmic cut in the interval $0 \le \omega \le 1$. There is no cut in the interval $-\infty < \omega < 0$ because we neglected the unphysical cut below q^2_{sk} in the ansatz (5) for the form factors. The poles in $f(x,\Omega)$, Eq. (18), at

$$\Omega = \pm \frac{i}{x}, \quad \text{i.e.} \quad \omega = \frac{x^2 \pm ix}{1+x^2} \tag{21}$$

show up only in the second sheet. They reflect the conjugate pair of dipoles built into the unphysical sheet of the excitation form factors G_k.

4) The scaling variable ω enters into the expressions (16) and (20) for the scaling functions only in the combination $\Omega = (\omega-1)/\omega$.

5) The scaling functions have the following threshold behaviour at $\omega = 1$

$$F_2(\omega) = N^2 \left(\ln x - \frac{\pi}{2} x\right)^2 \Omega^3 + O(\Omega^4 \ln^2\Omega), \tag{22}$$

$$\bar{F}_2(-\omega) = N^2 \left(\ln x - \frac{\pi}{2} x\right)^2 |\Omega|^3 + O(\Omega^4 \ln^2|\Omega|), \tag{23}$$

i.e., the leading terms at $\omega = 1$ are of the same type with identical coefficients. Apparently the Drell-Yan-West [7] relation is satisfied. The cut occurs in the non-leading terms.

6) For $\omega \to \infty$ $(\Omega \to 1)$ the deep inelastic scaling function $F_2(\omega)$ becomes constant thus simulating a possible Pomeron contribution which is compatible with present data.

7) Our model contains two free dimensionless parameters N and $\varkappa$ since the slope parameters α' and γ' of the trajectories of masses and widths occur only in the combination $\varkappa$ *). In the following we adjust N for every value of $\varkappa$ such that $F_2(\omega)$, Eq. (16), fits the experimental data at the point $\omega = 2$.

8) It is of some interest to look at the result for $\varkappa = 0$, corresponding to vanishing slope γ' of the trajectory of the widths. With $N \ln \varkappa \to N_0$ in the limit $\varkappa \to 0$ **) we obtain

$$F_2(\omega) = N_0^2 \left(\frac{\omega - 1}{\omega}\right)^3 , \quad (1 \leq \omega < \infty) , \tag{24}$$

$$\bar{F}_2(-\omega) = N_0^2 \left|\frac{\omega - 1}{\omega}\right|^3 , \quad (0 \leq \omega \leq 1) . \tag{25}$$

Obviously, in this limit the Drell-Levy-Yan [2] crossing relation is satisfied since this scaling function $F_2(\omega)$ does not possess a cut. In Fig. 2 $F_2(\omega)$, Eq. (24), is shown for two choices of N_0. The upper curve $(\varkappa = 0, \; N_0^2 = 0.981)$ has been adjusted to the experimental value at $\omega = 2$, the lower one $(\varkappa = 0, \; N_0^2 = 0.35)$ to the value 0.35 at infinity.

---

*) With the common value of about 1 GeV^{-2} for the Regge slope α' the parameter $\varkappa^2$ directly measures the slope γ' of the trajectory of the widths in units of GeV^2.

**) Since we fit N for every value of $\varkappa$ at a fixed value of ω the product $N \ln \varkappa$ remains finite for $\varkappa \to 0$. This is also necessary for finiteness of the form factors in this limit.

9) In Fig. 2 we compare the scaling function $F_2(\omega)$, Eq. (16), for different values of $\varkappa$ with the experimental data. Values of $\varkappa$ in the neighbourhood of 0.5 are favoured. In fact, the curve for $\varkappa = 0.5$ fits the data reasonably well.

10) With the values of N determined from the above fits of the deep inelastic scaling function $F_2(\omega)$ we obtain the predictions for the scaling function $\bar{F}_2(-\omega)$ in the deep annihilation region displayed in Fig. 3. It is obvious that the dependence on $\varkappa$ is appreciable, the values of $\bar{F}_2$ at fixed ω are different up to two orders of magnitude in the range of $\varkappa$ considered. In Fig. 4, we have redrawn the same curves over the abscissa $\ln|\omega - 1/\omega|$. This plot shows clearly that over a wide range in ω adjacent to $\omega = 1$ the leading term of all curves is proportional to $|\omega - 1/\omega|^3$. The curves for finite $\varkappa$ reach a maximum, the location of which is, except for the absolute value, the most distinctive feature. These maxima are caused by the complex poles of the form factors, as discussed under 3), Eq. (21).

For finite values of $\varkappa \neq 0$ the scaling function $\bar{F}_2(-\omega)$ vanishes for $\omega \to 0$ like

$$\bar{F}_2(-\omega) \sim \omega \ln^2 \omega , \tag{26}$$

whereas for $\varkappa = 0$ the scaling function diverges like ω^{-3} for $\omega \to 0$, Eq. (25).

11) Recently Callan and Gross [8] have emphasized that the behaviour at $\omega = 0$ of the scaling function $\bar{F}_2$ decides the type of growth of the average multiplicity $n(q^2)$ of hadrons produced in deep inelastic annihilation. One has for the scaling contribution for large q^2 *)

$$n(q^2) \approx \int_{2M/\sqrt{q^2}}^{1} d\omega\, \omega^2 \bar{F}_2(-\omega) . \tag{27}$$

---

*) It is assumed that the longitudinal scaling function vanishes and that the total annihilation cross-section behaves like q^{-2}.

Thus, according to Eq. (26) we predict for $\varkappa > 0$ a finite multiplicity, whereas for $\varkappa = 0$ the multiplicity will grow logarithmically in q^2 in this model.

12) As a last point we come to the decisive questions in a comparison with future colliding beam experiments.

a) Does scaling hold in the deep annihilation region, as predicted by this model?

b) Is the leading term in $\bar{F}_2(-\omega)$ which is proportional to $|\omega-1|^3/\omega^3$, a fit to the experimental data in the region $0.6 \lesssim \omega \leq 1$?

c) Do the experimental data show a maximum (instead of a ω^{-3} or worse divergence at $\omega \to 0$) leading to a finite multiplicity?

Obviously, the experiments will never reach the point $\omega = 0$. Therefore, conclusions about the multiplicity have to be drawn with care, since the model discussed in this paper shows that the deviation of $\bar{F}_2$ from its leading term $|\omega-1|^3/\omega^3$ at ω close to unity might occur at rather small values of ω. This would imply that the deviation from a logarithmically growing multiplicity may not be easily detectable.

It is interesting to note that the measurement of the location of the maximum of $\bar{F}_2$ can directly be translated into a value of $\varkappa$, which for a given Regge slope α' is a measurement of the slope γ' of the trajectory of the widths.

The above conclusions are independent of any assumption on light cone behaviour.

We thank P. Minkowski for an interesting discussion and C. Llewellyn Smith for reading the manuscript.

REFERENCES

1) H.D. Dahmen and F. Steiner, CERN TH.1595 (1972).

2) S.D. Drell, D.J. Levy and T.M. Yan, Phys.Rev. D1, 1617 (1970).

3) E.D. Bloom and F.J. Gilman, Phys.Rev.Letters 25, 1140 (1970).

4) G. Domokos, S. Kövesi-Domokos and E. Schonberg, Phys.Rev. D3, 1184 (1971).

5) M. Pavkovic, ICTP preprint No IC/69/118 (1969), unpublished;
M. Elitzur, Phys.Rev. D3, 2166 (1971).
H. Moreno and J. Pestieau, Phys.Rev. D5, 1210 (1972).

6) P.V. Landshoff and J.C. Polkinghorne, Nuclear Phys. B19, 432 (1970).

7) S.D. Drell and T.M. Yan, Phys.Rev.Letters 24, 181 (1970);
G.B. West, Phys.Rev. Letters 24, 1206 (1970).

8) C.G. Callan Jr., and D.J. Gross, Princeton preprint (1972);
P.V. Landshoff and J.C. Polkinghorne, DAMTP 72/38.

FIGURE CAPTIONS

Figure 1 :

Kinematics of the resonance exchange.

Figure 2 :

Plots of the scaling function F_2 in the deep inelastic region for different choices of $\varkappa$. The dashed lines indicate the asymptotic limit of the various curves.

Figure 3 :

Plots of the scaling functions $\bar{F}_2$ in the deep annihilation region for different choices of $\varkappa$.

Figure 4 :

Scaling functions $\bar{F}_2$ plotted against $\ell n \, |\omega - 1/\omega|$.

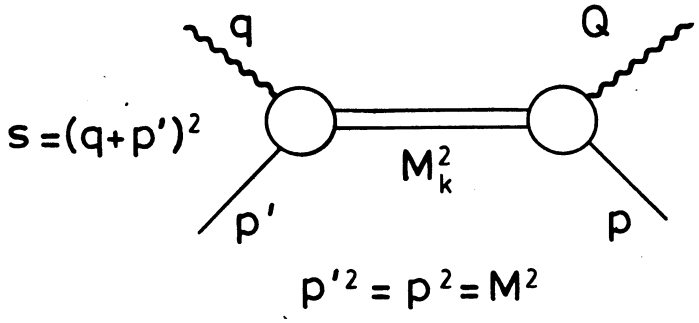

FIG.1

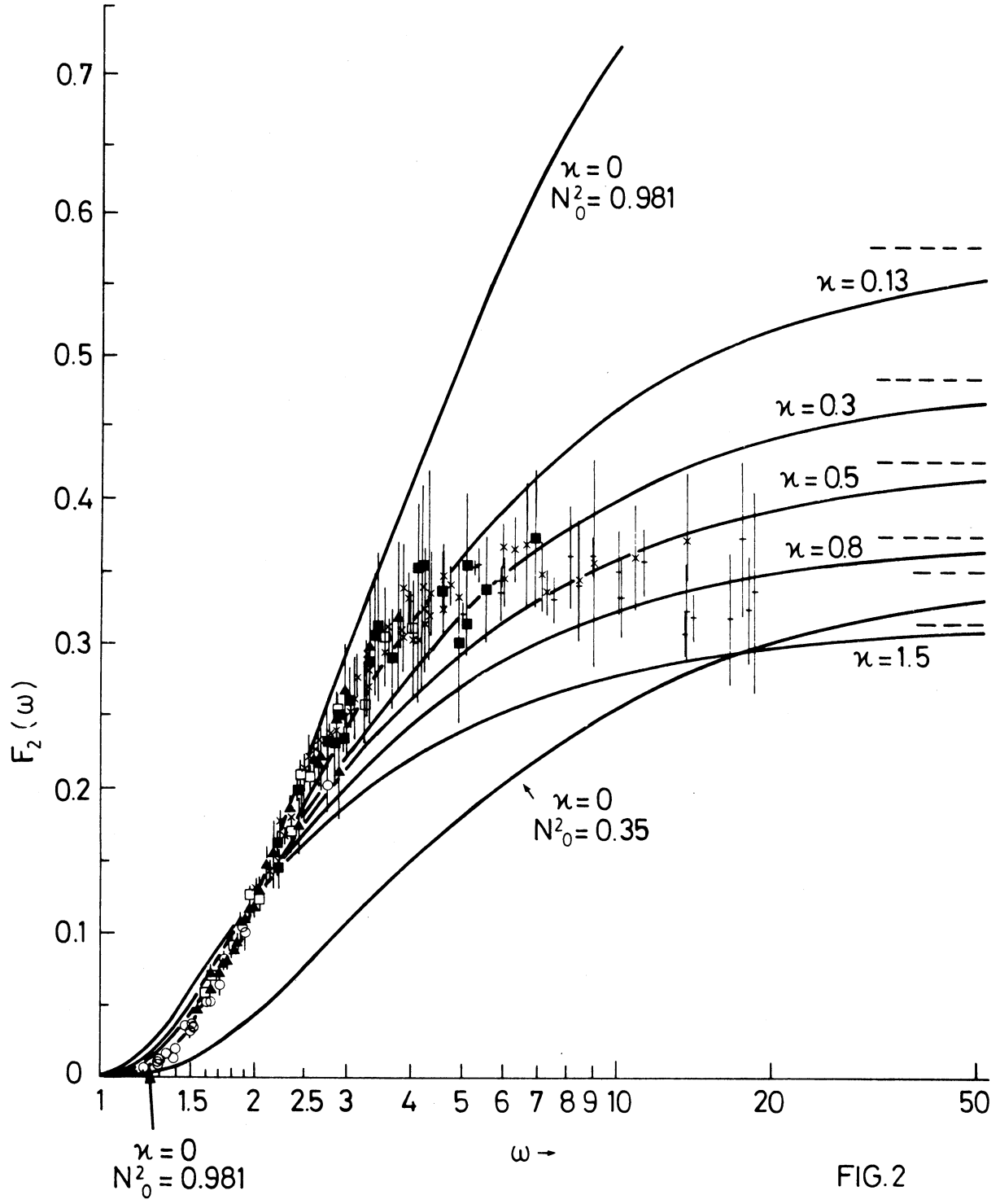
0.7
0.6
0.5
0.4
0.3
0.2
0.1
0
$F_2(\omega)$
$\varkappa = 0$
$N_0^2 = 0.981$
$\varkappa = 0.13$
$\varkappa = 0.3$
$\varkappa = 0.5$
$\varkappa = 0.8$
$\varkappa = 1.5$
$\varkappa = 0$
$N_0^2 = 0.35$
1
1.5
2
2.5
3
4
5
6
7
8
9
10
20
50
$\omega \rightarrow$
$\varkappa = 0$
$N_0^2 = 0.981$

FIG. 2

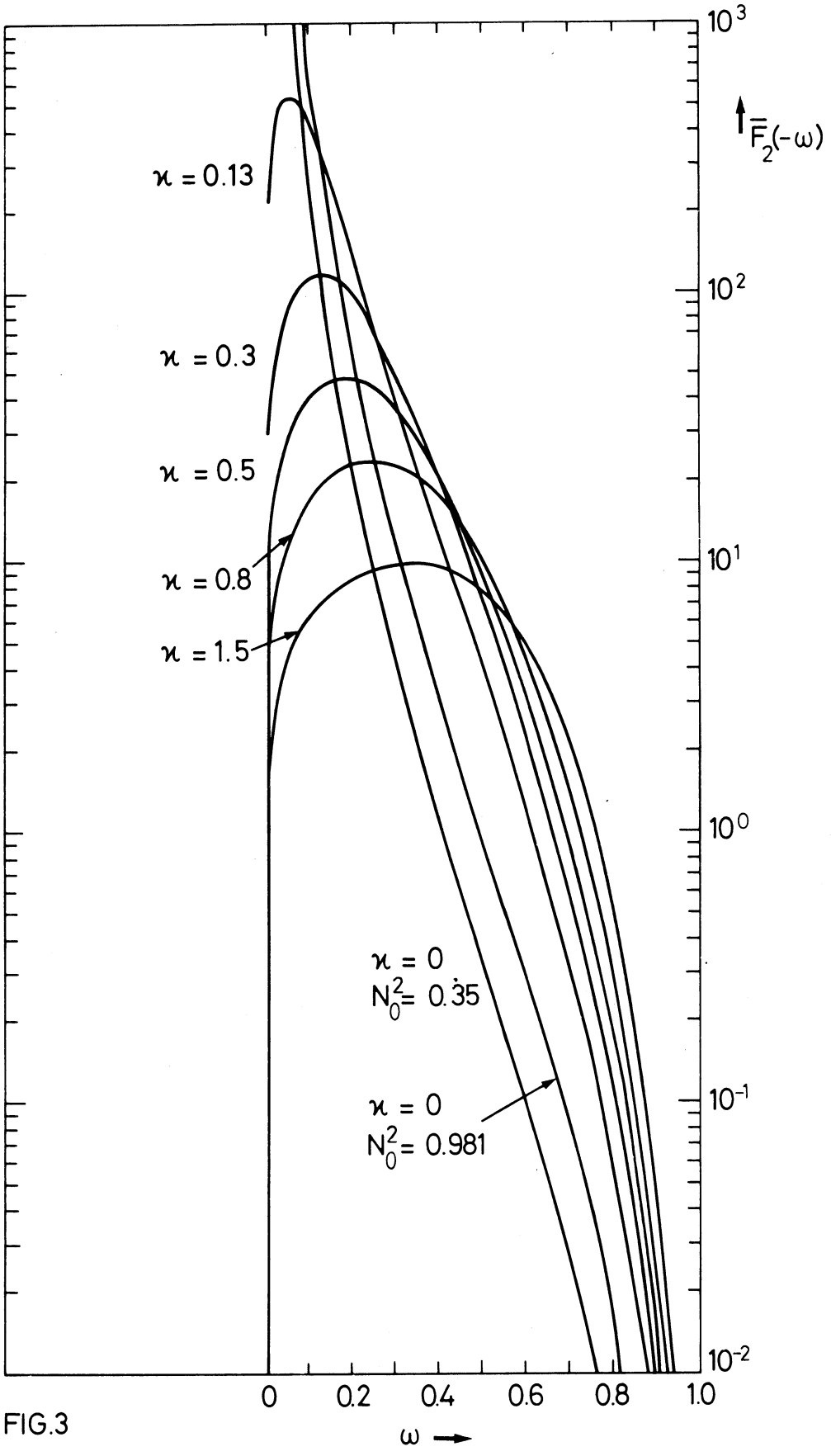
10^3
10^2
10^1
10^0
10^{-1}
10^{-2}
$\bar{F}_2(-\omega)$
$\varkappa = 0.13$
$\varkappa = 0.3$
$\varkappa = 0.5$
$\varkappa = 0.8$
$\varkappa = 1.5$
$\varkappa = 0$
$N_0^2 = 0.35$
$\varkappa = 0$
$N_0^2 = 0.981$
0
0.2
0.4
0.6
0.8
1.0
$\omega \rightarrow$

FIG.3

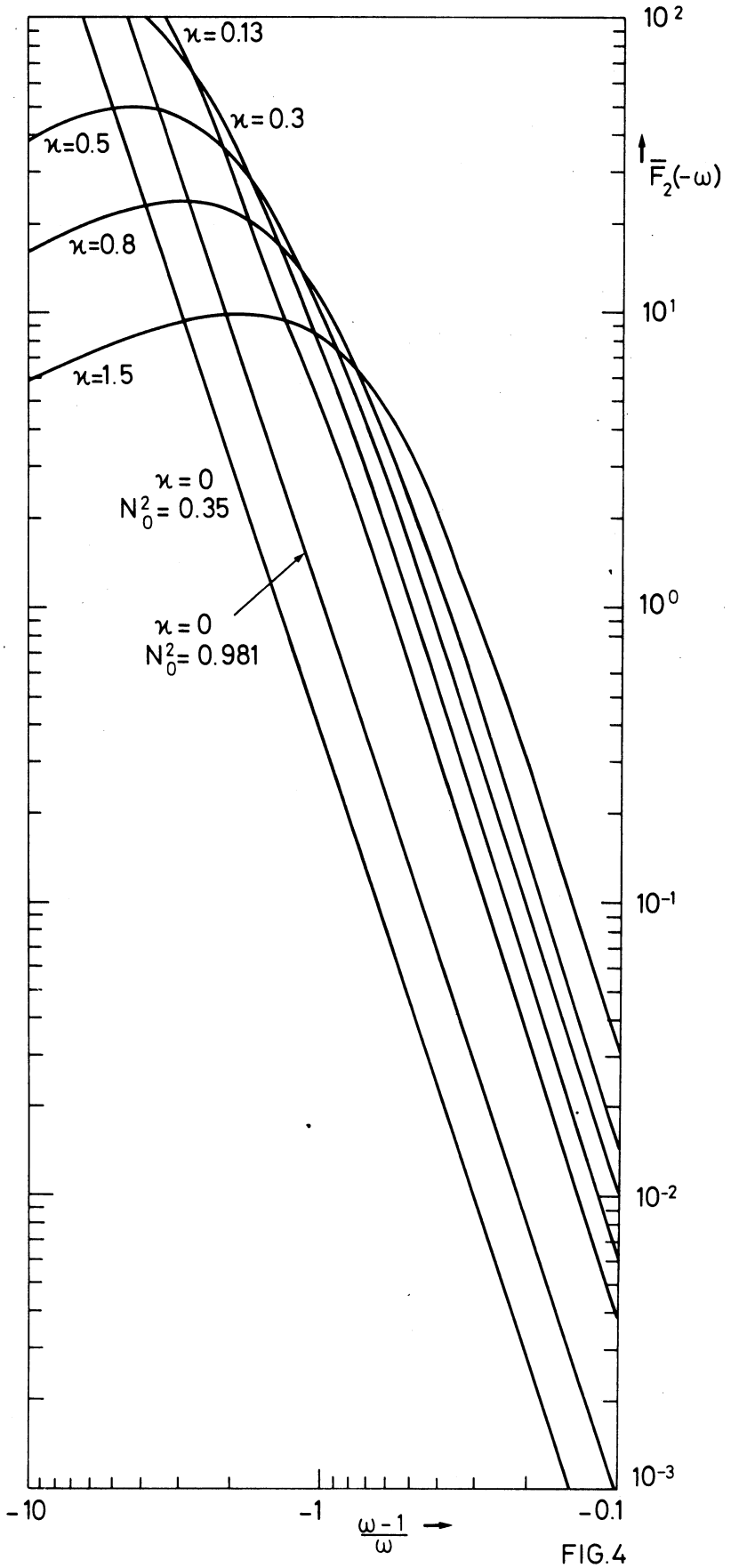
$\varkappa = 0.13$
$\varkappa = 0.3$
$\varkappa = 0.5$
$\varkappa = 0.8$
$\varkappa = 1.5$
$\varkappa = 0$
$N_0^2 = 0.35$
$\varkappa = 0$
$N_0^2 = 0.981$
10^2
10^1
10^0
10^{-1}
10^{-2}
10^{-3}
$\bar{F}_2(-\omega)$
-10
-1
-0.1
$\frac{\omega - 1}{\omega}$

FIG.4